Schizophrenia-associated differential DNA methylation in the superior temporal gyrus is distributed to many sites across the genome and annotated by the risk gene *MAD1L1*

Brandon C. McKinney[1,], Christopher M. Hensler[4], Yue Wei[2], David A. Lewis[1,4], Jiebiao Wang[2], Ying Ding[2], Robert A. Sweet[1,3,4].

University of Pittsburgh Departments of [1]Psychiatry, [2]Biostatistics, [3]Neurology, and [4]Translational Neuroscience Program, Pittsburgh, PA

For questions and correspondence, please contact Brandon C. McKinney, MD, PhD.

Mail: Biomedical Science Tower, Room W-1658
3811 O'Hara Street, Pittsburgh, PA 15213-2593

Express Mail: Biomedical Science Tower, Room W-1658
Lothrop and Terrace Streets, Pittsburgh, PA 15213-2593

Word Count

Abstract: 246
Body: 3170

ABSTRACT:

Background: Many genetic variants and multiple environmental factors increase risk for schizophrenia (SZ). SZ-associated genetic variants and environmental risk factors have been associated with altered DNA methylation (DNAm), the addition of a methyl group to a cytosine in DNA. DNAm changes, acting through effects on gene expression, represent one potential mechanism by which genetic and environmental factors confer risk for SZ and alter neurobiology.

Methods: We investigated the hypothesis that DNAm in superior temporal gyrus (STG) is altered in SZ. We measured genome-wide DNAm in postmortem STG from 44 SZ subjects and 44 non-psychiatric comparison (NPC) subjects using Illumina Infinium MethylationEPIC BeadChip microarrays. We applied tensor composition analysis to extract cell type-specific DNAm signals.

Results: We found that DNAm levels differed between SZ and NPC subjects at 242 sites, and 44 regions comprised of two or more sites, with a false discovery rate cutoff of q=0.1. We determined differential methylation at nine of the individual sites were driven by neuron-specific DNAm alterations. Glia-specific DNAm alterations drove the differences at two sites. Notably, we identied SZ-associated differential methylation within within mitotic arrest deficient 1-like 1 (*MAD1L1*), a gene strongly associated with SZ through genome-wide association studies.

Conclusions: This study adds to a growing number of studies that implicate DNAm, and epigenetic pathways more generally, in SZ. Our findings suggest differential methylation may contribute to STG dysfunction in SZ. Future studies to identify the mechanisms by

which altered DNAm, especially within MAD1L1, contributes to SZ neurobiology are warranted.

INTRODUCTION:

Schizophrenia (SZ) is a severe neuropsychiatric disorder with complex etiology. Heritability estimates for SZ from twin studies are consistently ~80% (1), thus suggesting a substantial genetic contribution to its etiology. Genome-wide association studies (GWAS) have identified many common variants associated with SZ, although each variant has only a small effect on risk for the disorder (2). A recent large-scale GWAS meta-analysis identified such variants at 145 distinct genetic loci (3). Heritability estimates from GWAS fall short of those predicted by twin studies, thus suggesting that other forms of genetic variation contribute risk for SZ. Indeed, recent studies have found a high burden of both rare single nucleotide variants and rare copy number variants in subjects with SZ (4,5). Multiple environmental factors have also been found to contribute to SZ etiology including, among others, maternal infections and malnutrition during pregnancy and obstetric complications (6).

SZ-associated genetic variation and environmental factors associated with SZ risk have both been found to alter DNA methylation (DNAm) (7–11). DNAm, the addition of a methyl group to a cytosine in DNA, stably affects gene experession via interaction with transcription factor binding (12). DNAm is associated with both increased and decreased gene expression as well as other forms of gene regulation, including splicing and alternative promoter usage (12–14). Changes in DNAm, acting through effects on gene expression, represent one potential mechanism by which both genetic and environmental factors can confer risk for SZ and alter brain development and biology.

The superior temporal gyrus (STG) is a region of the brain critical for auditory processing. In individuals with SZ, altered STG function is associated with auditory verbal hallucinations and impaired auditory sensory processing . Impaired auditory processing further contributes to phonologic dyslexia and difficulty recognizing and expressing spoken emotional tone (prosody) in SZ (15). In this study, we investigated the hypothesis that DNAm is altered in the STG from subjects with SZ. To this end, we used Illumina Infinium MethylationEPIC BeadChip microarrays (EPIC arrays) to measure genome-wide DNAm in the STG from 44 subjects with SZ and 44 non-psychiatric comparison (NPC) subjects. Tensor composition analysis (TCA) was used to extract cell type-specific DNAm signals from brain tissue-level data.

MATERIALS AND METHODS:

POSTMORTEM BRAINS

Tissue was obtained from postmortem brains recovered and processed as described previously (16,17). Briefly, brains were retrieved during routine autopsies at the Allegheny County Medical Examiner's Office, Pittsburgh, PA, USA, following informed consent from next-of-kin. An independent committee of experienced clinicians made consensus Diagnostic and Statistical Manual of Mental Disorders, Fourth Edition diagnoses, or determined the absence thereof, based on clinical records and collateral history obtained via structured interviews with surviving relatives (18). The right hemisphere was blocked coronally and the resultant slabs snap frozen and stored at -80°C. Slabs containing the STG were identified and the STG was removed as a single block from each of the slabs in which it was present. Samples containing all six cortical layers of STG (planum

temporale), but excluding the adjacent white matter, were harvested. All procedures were approved by the University of Pittsburgh Committee for the Oversight of Research and Clinical Training Involving Decedents and the Institutional Review Board for Biomedical Research.

COHORT MEMBERSHIP

The cohort comprised 44 subjects with either schizophrenia (N=31) or schizoaffective disorder (N=13), and 44 NPC subjects. Subjects diagnosed with schizophrenia and schizoaffective disorder were grouped together for analysis, and referred to as SZ subjects, or the SZ group. In this manuscript, as in our previous studies, we found that the diagnoses do not differ with respect to DNAm (19). Each subject in the SZ group was matched with one NPC subject for sex, hemisphere, and as closely as possible for postmortem interval (PMI), age, and other characteristics (Table 1 and Supplementary Table 1).

DNA PREPARATION AND BISULFITE CONVERSION

DNA (~10 ug) was isolated from STG gray matter (~20 mg) using AllPrep DNA/RNA/Protein Mini Kit (Qiagen, Valencia, CA, USA) and bisulfite converted using EZ-96 DNA Methylation Kit (Zymo Research, Irvine, CA, USA), both as per manufacturer's protocol.

DNA METHYLATION ARRAYS

DNAm is the addition of a methyl group to a cytosine in DNA. DNAm is observed within the context of cytosine-phosphate-guanine dinucleotides (CpGs), most commonly, but also within the context of a cytosine-phosphate-H dinucleotides (CpHs; H=cytosine, adenine, thymine) (20,21). CpGs and CpHs are referred to as 'DNAm sites' or 'sites' in this manuscript. DNAm was measured at 866,091 sites using MethylationEPIC BeadChip Infinium array (EPIC array; Illumina, San Diego, CA, USA) as per manufacturer's protocol (22,23). A *β*-value, the proportion of a particular site that is methylated in a DNA sample, was determined for each site by taking the ratio of the methylated to unmethylated signal, using the formula: *β*-value = intensity of the methylated signal/(intensity of the unmethylated signal + intensity of the methylated signal + 100). A 96-entry EPIC array was filled with samples from the 88 subjects, including replicate samples from eight subjects. Data is available for download from Gene Expression Omnibus (GEO; GSE144910).

DATA PREPROCESSING AND FILTERING

Data analyses were performed using the R software environment (www.r-project.org). Color adjustment and background correction were performed using the bgAdjust2C method (24). Normalization was performed using the *preprocessQuantile* function in the R package *minfi* (25). The initial dataset comprised data from 1,051,815 probes corresponding to 866,091 DNAm sites for each subject. Multidimensional scaling (MDS) was used to visualize the degree of similarity among samples (26). Prior to data filtering, samples segregated strongly by sex in MDS space (Supplemental Figure 1A). Data filtering involved removing all data points associated with a probe if the probe failed

detection as indicated by a median detection p-value >0.01 (probes corresponding to 12,350 DNAm sites), cross-reacted with multiple genomic regions (probes corresponding to 39,269 DNAm sites), contained a single nucleotide polymorphism within its binding site (probes corresponding to 27,395 DNAm sites), or interrogated a DNAm site on a sex chromosome (probes corresponding to 18,628 DNAm sites). Data from probes corresponding to 768,449 DNAm sites remained for downstream analysis (Supplemental Figure 2). After data filtering, MDS using data from the 3,000 most variable sites was performed and samples no longer segregated by sex (Supplemental Figure 1B), but segregation by race (Supplemental Figure 1C) and age (Supplemental Figures 1D and 1E) became evident. The replicate sample pairs from each of the eight subjects from which replicate samples were collected and assayed co-segregated in MDS space (Supplemental Figure 1F), thus demonstrating the reproduceability of our approach. The β-values for each replicate pair were averaged for the downstream analyses.

DIFFERENTIAL DNA METHYLATION

Linear regression was used to identify differentially methylated sites (DMSs). DNAm, in the form of preprocessed and normalzed β-values, was the dependent variable and diagnosis was the independent variable. Race, age, and PMI were included as covariates in the analysis. The MDS analysis described above supported the inclusion of race as a covariate. Most subjects in this cohort self-identifed as either white or black, however, one subject self-identified as Asian Indian and, consistent with known genetic architecture (27), clustered with the subjects of European ancestry (Supplemental Figure 1C) and was thus combined with the subjects that self-identified as white for analyses. The inclusion

of age as a covariate is supported by the MDS analysis as well as existing literature that shows age has a robust effect on DNAm (28–30). Though samples did not segregate by PMI in MDS space (data not shown), it was included as a covariate because the stability of many molecular measures have been found to be particularly sensitive to PMI (31,32), and to maintain consistency with our previous study in which it was included as a covariate in our primary analyses (19).

Differential methylated regions (DMRs) were identified using the R package DMRcate (33). DMRcate uses an approach based on tunable kernel smoothing of the differential methylation signal across the genome obtained in the site-based differential DNAm analysis described above. A Benjamini–Hochberg corrected false discovery rate (FDR) <0.1 for the smoothed signal was considered significant. Then regions with a maximum of 1000 basepairs containing at least two such significant sites were defined as DMRs.

NEURON AND GLIA PROPORTION ESTIMATES

The proportion of neurons and glia in each sample was estimated with CETS, an R package that uses β-values from cell type-specific sites to generate the estimation (34).

NEURON- AND GLIA-SPECIFIC DIFFERENTIAL DNA METHYLATION

The CETS-estimated proportions of neurons and glia for each subject and tensor composition analysis (TCA) (35) were used to estimate the subject-level neuron- and glia-specific β-values for each DNAm site and detect sites at which DNAm differs between

subjects with SZ and NPC subjects. The cell type proportions were refit in TCA and adjusted for age, race, and PMI.

RESULTS:

SZ-associated differential DNA methylation was identified at many individual sites and genomic regions.

DNAm differed between subjects with SZ and NPC subjects at more sites than would be expected by chance (Figure 1A). DNAm differed at 242 sites between subjects with SZ and NPC subjects with an FDR cutoff of q=0.1 (Table 2). Of these 242 differntially methylated sites (DMSs), DNAm differed at 101 with a FDR cutoff of q=0.05. No global differences in DNAm were identified between SZ and NPC subjects (Supplemental Figure 3). The sites at which DNAm differed between subjects with SZ and NPC subjects were broadly distributed across all autosomes (Figure 1B).

DNAm is known to differ markedly between neurons and glia (36), and detection of DNAm differences between groups in tissue with multiple cell types can be confounded by cell composition. In STG samples studied here, neuronal proportion did not differ between subjects with SZ and NPC subjects (SZ=0.46±0.05; NPC=0.46±0.04; p=0.50) (Supplemental Table 2A), and we have previously shown that pyramidal neuron number in layer 3 of this brain region did not differ between subjects with SZ and NPC subjects (37). After adjusting for neuron proportion, DNAm differed at 256 sites between SZ and NPC subjects with the FDR cutoff of q=0.1 (Supplemental Table 2B). Of these 256 sites, 210 were among the 242 detected prior to adjusting for neuron proportion thus suggesting

that cell composition does not account for the majority of observed differences in DNAm.

Genomic regions in which DNAm at multiple contiguous sites differs between SZ and NPC subjects, or differentially methylated regions (DMRs), may be more biologically meaningful or have different functional consequences than those of a single DMS. There were 44 genomic regions in which DNAm at two or more contiguous, measured sites differed between subjects with SZ and NPC subjects (Table 3).

Of note, three DMSs and one DMR were identified within mitotic arrest deficient 1-like 1 (*MAD1L1*), a gene strongly associated with SZ through genome-wide association studies (3). The *MAD1L1*-associated differential methylation we identified spanned a portion of intron 2 and exon 3, and the DNAm levels were lower in SZ subjects relative to NPC subjects.

SZ-associated differential DNA methylation at some individual sites was specific to neurons or glia

Cell type deconvolution identified nine differentially methylated sites in neurons (Figure 2A and 2C) and two differentially methylated sites in glia (Figure 2B and 2C) with an FDR cutoff of q=0.1. All 11 sites for which DNAm differed between SZ and NPC subjects in cell type-specific manner were also identified as being differentially methylated in the bulk tissue analysis (Table 2).

DISCUSSION:

In the STG of SZ subjects, we indentified DNAm differences at 242 individual sites and 44 genomic regions with multiple sites. Notably, we found SZ-associated differential methylation in *MAD1L1*, a gene that harbors a single nucleotide polymorphism (SNP) that strongly associates with SZ (third out of 145 loci that reached genome-wide significance) in the largest meta-analysis of genome-wide association studies to date from the Schizophrenia Working Group of the Psychiatric Genomics Consortium (3). The *MAD1L1*-associated differential methylation we identified was characterized by lower DNAm in SZ subjects relative to NPC subjects, a difference we determined to be driven by neuron-specific alterations in DNAm. This finding is consistent with studies in the prefrontal cortex that also identified genome-wide significant DMRs in MAD1L1 (10).

Despite strong evidence implicating *MAD1L1* in SZ, the underlying mechanisms through which MAD1L1-associated SNPs and differential methylation might contribute to SZ neurobiology are unclear. MAD1L1 is expressed in many human tissues (39,40), and is known to have a role in regulating the spindle assembly checkpoint during mitosis (41). Genetic mutations that disrupt MAD1L1 expression are associated with aneuploidy and multiple cancers (39,40). During development MAD1L1 is most strongly expressed in differentiating cells and is critical for the transition from proliferation to terminal differentiation in a broad range of cell types (42,43). Given MAD1L1 is expressed in both neurons and glia of most brain regions (44–46), the differentiation of neurons and glia may be disrupted if MAD1L1 expression is affected by SZ-associated differential methylation during neurodevelopment. Such a disruption would be predicted to alter the delicate balance of the various neuronal and glia subtypes and thus brain circuitry,

perhaps giving rise to the dysfunctional brain circuits that are associated with the clinical features of SZ (47).

Alternatively, MAD1L1 may act post-neurodevelopment as its expression in terminally differentiated cells, including post-mitotic neurons and glia, suggests a function in addition to those related to development. Studies have found that its expression in terminally differentiated cells may be necessary for maintaining the differentiated state (48–50). Indeed, even modest decreases in MAD1L1 expression leads to dedifferentiation in some cell types (48). Some evidence points to a role for dedifferentiation of post-mitotic neurons in the cognitive decline and behavioral changes associated with normal brain aging in humans (51–53), and a similar mechanism could conceivably contribute to SZ neurobiology. That said, these proposed mechanisms are conjecture and critical next steps should focus on understanding MAD1L1 in the brain, generally, and translating MAD1L1-associated SNPs and differential methylation into molecular mechanisms for SZ, specifically.

This study is the first to identify SZ-associated differential methylation in the STG. Others have previously reported DNAm differences between subjects with SZ and NPC subjects in the prefrontal cortex (10,38,54–56), striatum (54), hippocampus (54,57), and cerebellum (54) thus suggesting that altered DNAm in multiple brain regions contributes to SZ neurobiology. Our findings add to the growing body of literature that implicates altered epigenetic pathways, including DNAm as well as histone modifications (58–60), in SZ neurobiology. Though most often studied separately, there is extensive crosstalk

between DNAm and histone modification pathways (61–63). This crosstalk drives the establishment of composite epigenetic signatures that depend on epigenetic regulatory enzymes (e.g., DNA methyltransferases, histone methyltransferases, etc) with protein domains that specifically recognize methylated DNA and/or modified histones and thus allow for linking of DNAm and histone modifications at appropriate sites in the genome. SETD1A, a gene in which loss-of-function mutations confer a large increase in risk for SZ (64), is an example of an enzyme linking DNAm and histone modification. SETD1A methylates histones after it is localized to unmethylated DNA via an interaction with CXXC-finger protein-1 (65). This body of literature suggests that a more complete understanding of how these epigenetic pathways and their interactions are altered in SZ is likely to be fruitful in identifying molecular mechanisms contributing to SZ. Epigenetic editing technologies that use highly specific DNA-targeting tools (e.g., CRISPR) to methylate DNA or modify histones in a locus-specific manner will be valuable in dissecting these molecular mechanisms in cell culture and animal models (66,67).

Our findings in this study, like those of all postmortem brain studies, are only correlative and cannot establish causal relationships. The causes of the SZ-associated differences in DNAm that we identified in the STG are likely a combination of genetic and environmental factors. Methylation quantitative trait loci are common genetic variants that influence DNAm levels at sites in a particular genomic region, and they are common in the brain (68). However, none of the differentially methylated loci identified in this study have been shown to be associated with genetic variants that overlap with SZ risk loci

(10,54), or are known to be altered by environmental risk factors for SZ like perinatal famine (11).

Though differential methylation may be associated with SZ risk factors, it may be the result of exposure to antipsychotics or others confounds. Studies of peripheral tissues indicate that antipsychotics do alter DNAm (69). However, DNAm alterations are already present in subjects with only brief (<16 weeks) antipsychotic treatment (70), thus suggesting that much SZ-associated differential methylation is intrinisic to the illness. Some studies have even found that SZ-associated DNAm alterations in peripheral tissues are normalized by treatment with antipsychotics (71), raising the possibility that the therapeutic effects of antipsychotics are mediated, in part, by DNAm changes. Such findings also make it likely that antipsychotics mask some SZ-associated differential methylation from being detected in studies.

An additional potential confound particularly relevant in studies of DNAm in subjects with SZ is cigarette smoking. Cigarette smoking is much more common among individuals with SZ than the general population and is known to induce robust DNAm changes in peripheral tissues (72). The effect of cigarette smoking on DNAm in the brain has not been studied. However, none of the differentially methylated sites or regions identified in this study have been found to be among the sites most strongly affected by cigarette smoking in peripheral tissues.

This study lays the groundwork for more detailed investigations of SZ-associated differential methylation in the STG. Future studies should focus identifying the mechanisms by which altered DNAm, especially within MAD1L1, contributes to SZ neurobiology. To this end, studies that use of epigenetic editing technology to recapitulate SZ-associated differential methylation in cell cultures and animal models will be useful. Also of value will be studies that use a multi-omics approach for understanding the dynamic interaction among epigenome, transcriptome, and genetic variation in the STG.

FUNDING AND DISCLOSURES:

This work was supported by NIH Grants K23 MH112798 (BCM) and R01 MH071533, MH116046, and AG027224 (RAS). The content is solely the responsibility of the authors and does not necessarily represent the official views of the National Institutes of Health, or the United States Government. DAL currently receives investigator-initiated research support from Pfizer and Merck. All the other authors declare no competing interests.

FIGURE LEGENDS:

Figure 1. SZ-associated differential methylation. (A) Probability plot showing that the analysis for sites at which DNAm differed between SZ and NPC subjects is enriched in small p-values compared to what would be expected by chance. The y=x line represents the distribution of p-values than would be expected by chance. **(B)** Manhattan plot showing that the DNAm differed between subjects with SZ and NPC subjects at many DNAm sites, and the sites were distributed across many autosomes. The horizontal lines represent FDR cutoff of q=0.1 (bottom) and q=0.05 (top). DNAm, DNA methylation; SZ,

schizophrenia; NPC, non-psychiatric comparison; FDR, false discovery rate.

Figure 2. Neuron- or glia-specific differential methylation in SZ . (A) Manhattan plot showing neuron-specific DNAm differences between SZ and NPC subjects at nine sites. **(B)** Manhattan plot showing glia-specific DNAm differences between SZ and NPC subjects at two sites. **(C)** Box plots of DNAm (*β*-value) at sites of cell type-specific differences in DNAm between SZ and NPC subjects. DNAm, DNA methylation; SZ, schizophrenia; NPC, non-psychiatric comparison.

REFERENCES:

1. Hilker R, Helenius D, Fagerlund B, Skytthe A, Christensen K, Werge TM, et al. Heritability of Schizophrenia and Schizophrenia Spectrum Based on the Nationwide Danish Twin Register. Biol Psychiatry. 2018;
2. Ripke S, Neale BM, Corvin A, Walters JTR, Farh KH, Holmans PA, et al. Biological insights from 108 schizophrenia-associated genetic loci. Nature. 2014;511(7510):421–7.
3. Pardiñas AF, Holmans P, Pocklington AJ, Escott-Price V, Ripke S, Carrera N, et al. Common schizophrenia alleles are enriched in mutation-intolerant genes and in regions under strong background selection. Nat Genet. 2018;
4. Genovese G, Fromer M, Stahl EA, Ruderfer DM, Chambert K, Landén M, et al. Increased burden of ultra-rare protein-altering variants among 4,877 individuals with schizophrenia. Nat Neurosci. 2016;
5. Marshall CR, Howrigan DP, Merico D, Thiruvahindrapuram B, Wu W, Greer DS, et al. Contribution of copy number variants to schizophrenia from a genome-wide study of 41,321 subjects. Nat Genet. 2017;
6. Van Os J, Rutten BPF, Poulton R. Gene-environment interactions in schizophrenia: Review of epidemiological findings and future directions. Schizophrenia Bulletin. 2008.
7. Tobi EW, Goeman JJ, Monajemi R, Gu H, Putter H, Zhang Y, et al. DNA methylation signatures link prenatal famine exposure to growth and metabolism. Nat Commun. 2014;
8. Heijmans BT, Tobi EW, Stein AD, Putter H, Blauw GJ, Susser ES, et al.

Persistent epigenetic differences associated with prenatal exposure to famine in humans. Proc Natl Acad Sci U S A. 2008;

9. Hannon E, Spiers H, Viana J, Pidsley R, Burrage J, Murphy TM, et al. Methylation QTLs in the developing brain and their enrichment in schizophrenia risk loci. Nat Neurosci [Internet]. 2016;19(1):48–54. Available from: http://www.ncbi.nlm.nih.gov/pubmed/26619357
10. Jaffe AE, Gao Y, Deep-Soboslay A, Tao R, Hyde TM, Weinberger DR, et al. Mapping DNA methylation across development, genotype and schizophrenia in the human frontal cortex. Nat Neurosci [Internet]. 2016;19(1):40–7. Available from: http://www.ncbi.nlm.nih.gov/pubmed/26619358
11. Boks MP, Houtepen LC, Xu Z, He Y, Ursini G, Maihofer AX, et al. Genetic vulnerability to DUSP22 promoter hypermethylation is involved in the relation between in utero famine exposure and schizophrenia. npj Schizophr. 2018;
12. Jones PA. Functions of DNA methylation: Islands, start sites, gene bodies and beyond. Nature Reviews Genetics. 2012.
13. Wagner JR, Busche S, Ge B, Kwan T, Pastinen T, Blanchette M. The relationship between DNA methylation, genetic and expression inter-individual variation in untransformed human fibroblasts. Genome Biol. 2014;
14. Maunakea AK, Nagarajan RP, Bilenky M, Ballinger TJ, Dsouza C, Fouse SD, et al. Conserved role of intragenic DNA methylation in regulating alternative promoters. Nature. 2010;
15. Javitt DC, Sweet RA. Auditory dysfunction in schizophrenia: integrating clinical and basic features. Nat Rev Neurosci [Internet]. 2015;16(9):535–50. Available

from: http://www.ncbi.nlm.nih.gov/pubmed/26289573

16. Sweet RA, Henteleff RA, Zhang W, Sampson AR, Lewis DA. Reduced dendritic spine density in auditory cortex of subjects with schizophrenia. Neuropsychopharmacology. 2009;34(2):374–89.

17. Glantz LA, Lewis DA. Decreased dendritic spine density on prefrontal cortical pyramidal neurons in schizophrenia. Arch Gen Psychiatry [Internet]. 2000;57(1):65–73. Available from: http://eutils.ncbi.nlm.nih.gov/entrez/eutils/elink.fcgi?dbfrom=pubmed&id=10632234&retmode=ref&cmd=prlinks%5Cnpapers3://publication/uuid/44227C59-6608-40A9-92C8-D27EF1BA4713

18. DSM-IV-TR. Diagnostic and statistical manual of mental disorders: DSM-IV-TR. DSM-V. 2000.

19. McKinney B, Ding Y, Lewis DA, Sweet RA. DNA methylation as a putative mechanism for reduced dendritic spine density in the superior temporal gyrus of subjects with schizophrenia. Transl Psychiatry [Internet]. 2017 Feb 14 [cited 2017 Jun 4];7(2):e1032. Available from: http://www.ncbi.nlm.nih.gov/pubmed/28195572

20. Nestler EJ, Peña CJ, Kundakovic M, Mitchell A, Akbarian S. Epigenetic Basis of Mental Illness. Neuroscientist. 2016;22(5):447–63.

21. Moore LD, Le T, Fan G. DNA methylation and its basic function. Neuropsychopharmacology. 2013 Jan;38(1):23–38.

22. Pidsley R, Zotenko E, Peters TJ, Lawrence MG, Risbridger GP, Molloy P, et al. Critical evaluation of the Illumina MethylationEPIC BeadChip microarray for whole-genome DNA methylation profiling. Genome Biol. 2016 Dec;17(1):208.

23. Moran S, Arribas C, Esteller M. Validation of a DNA methylation microarray for 850,000 CpG sites of the human genome enriched in enhancer sequences. Epigenomics [Internet]. 2016 Mar;8(3):389–99. Available from: http://www.ncbi.nlm.nih.gov/pubmed/26673039

24. Du P, Kibbe WA, Lin SM. lumi: a pipeline for processing Illumina microarray. Bioinformatics [Internet]. 2008;24(13):1547–8. Available from: http://www.ncbi.nlm.nih.gov/pubmed/18467348

25. Aryee MJ, Jaffe AE, Corrada-Bravo H, Ladd-Acosta C, Feinberg AP, Hansen KD, et al. Minfi: a flexible and comprehensive Bioconductor package for the analysis of Infinium DNA methylation microarrays. Bioinformatics. 2014 May;30(10):1363–9.

26. Cox TF, Cox MAA. Multidimensional scaling. Chapman & Hall/CRC; 2001. 308 p.

27. Xing J, Watkins WS, Shlien A, Walker E, Huff CD, Witherspoon DJ, et al. Toward a more uniform sampling of human genetic diversity: a survey of worldwide populations by high-density genotyping. Genomics [Internet]. 2010 Oct;96(4):199–210. Available from: http://www.ncbi.nlm.nih.gov/pubmed/20643205

28. Horvath S. DNA methylation age of human tissues and cell types. Genome Biol. 2013;

29. McKinney BC, Lin C-W, Rahman T, Oh H, Lewis DA, Tseng G, et al. DNA methylation in the human frontal cortex reveals a putative mechanism for age-by-disease interactions. Transl Psychiatry. 2019;9(1):39.

30. Akbarian S, Beeri MS, Haroutunian V. Epigenetic determinants of healthy and diseased brain aging and cognition. JAMA Neurol. 2013 Jun;70(6):711–8.

31. Lewis DA. The human brain revisited: opportunities and challenges in postmortem studies of psychiatric disorders. Neuropsychopharmacology [Internet]. 2002;26(2):143–54. Available from: http://www.ncbi.nlm.nih.gov/pubmed/11790510

32. McCullumsmith RE, Hammond JH, Shan D, Meador-Woodruff JH. Postmortem brain: an underutilized substrate for studying severe mental illness. Neuropsychopharmacology [Internet]. 2014 Jan;39(1):65–87. Available from: http://www.ncbi.nlm.nih.gov/pubmed/25767083

33. Peters TJ, Buckley MJ, Statham AL, Pidsley R, Samaras K, V Lord R, et al. De novo identification of differentially methylated regions in the human genome. Epigenetics and Chromatin. 2015;

34. Guintivano J, Aryee MJ, Kaminsky ZA. A cell epigenotype specific model for the correction of brain cellular heterogeneity bias and its application to age, brain region and major depression. Epigenetics [Internet]. 2013;8(3):290–302. Available from: http://www.ncbi.nlm.nih.gov/pubmed/23426267

35. Rahmani E, Schweiger R, Rhead B, Criswell LA, Barcellos LF, Eskin E, et al. Cell-type-specific resolution epigenetics without the need for cell sorting or single-cell biology. Nat Commun. 2019;

36. Kozlenkov A, Roussos P, Timashpolsky A, Barbu M, Rudchenko S, Bibikova M, et al. Differences in DNA methylation between human neuronal and glial cells are concentrated in enhancers and non-CpG sites. Nucleic Acids Res [Internet]. 2014 Jan;42(1):109–27. Available from: http://www.ncbi.nlm.nih.gov/pubmed/24057217

37. Dorph-Petersen KA, Delevich KM, Marcsisin MJ, Zhang W, Sampson AR,

Gundersen HJG, et al. Pyramidal neuron number in layer 3 of primary auditory cortex of subjects with schizophrenia. Brain Res [Internet]. 2009;1285:42–57. Available from: http://www.ncbi.nlm.nih.gov/pubmed/19524554

38. Wockner LF, Noble EP, Lawford BR, Young RM, Morris CP, Whitehall VL, et al. Genome-wide DNA methylation analysis of human brain tissue from schizophrenia patients. Transl Psychiatry [Internet]. 2014;4:e339. Available from: http://www.ncbi.nlm.nih.gov/pubmed/24399042

39. Sun Q, Zhang X, Liu T, Liu X, Geng J, He X, et al. Increased expression of mitotic arrest deficient-like 1 (MAD1L1) is associated with poor prognosis and insensitive to taxol treatment in breast cancer. Breast Cancer Res Treat. 2013;

40. Tsukasaki K, Miller CW, Greenspun E, Eshaghian S, Kawabata H, Fujimoto T, et al. Mutations in the mitotic check point gene, MAD1L1, in human cancers. Oncogene. 2001;

41. Amon A. The spindle checkpoint. Curr Opin Genet Dev. 1999;

42. Hurlin PJ, Foley KP, Ayer DE, Eisenman RN, Hanahan D, Arbeit JM. Regulation of Myc and Mad during epidermal differentiation and HPV-associated tumorigenesis. Oncogene. 1995;

43. Ohta Y, Hamada Y, Saitoh N, Katsuoka K. Effect of the transcriptional repressor Mad1 on proliferation of human melanoma cells. Exp Dermatol. 2002;

44. Cichon S, Mühleisen TW, Degenhardt FA, Mattheisen M, Miró X, Strohmaier J, et al. Genome-wide association study identifies genetic variation in neurocan as a susceptibility factor for bipolar disorder. Am J Hum Genet. 2011;

45. Hawrylycz MJ, Lein ES, Guillozet-Bongaarts AL, Shen EH, Ng L, Miller JA, et al.

An anatomically comprehensive atlas of the adult human brain transcriptome. Nature. 2012;

46. GTEx Project. GTEx portal. GTEx Analysis Release V6p (dbGaP Accession phs000424.v6.p1). 2017.

47. Lewis DA, Sweet RA. Schizophrenia from a neural circuitry perspective: advancing toward rational pharmacological therapies. J Clin Invest [Internet]. 2009;119(4):706–16. Available from: http://www.ncbi.nlm.nih.gov/pubmed/19339762

48. Han S, Park K, Kim HY, Lee MS, Kim HJ, Kim YD, et al. Clinical implication of altered expression of Mad1 protein in human breast carcinoma. Cancer. 2000;

49. Pan L, Zhang X, Suo X, Wang F, Niu Z, Dong Z. Expression and Mutation Analysis of the Myc Antagonist Gene Mad1 in Acute Leukemia. Blood. 2006;

50. Foley KP, Eisenman RN. Two MAD tails: What the recent knockouts of Mad1 and Mxi1 tell us about the MYC/MAX/MAD network. Biochimica et Biophysica Acta - Reviews on Cancer. 1999.

51. Oh G, Ebrahimi S, Wang SC, Cortese R, Kaminsky ZA, Gottesman II, et al. Epigenetic assimilation in the aging human brain. Genome Biol [Internet]. 2016;17:76. Available from: http://www.ncbi.nlm.nih.gov/pubmed/27122015

52. Koen JD, Rugg MD. Neural Dedifferentiation in the Aging Brain. Trends in Cognitive Sciences. 2019.

53. Park DC, Polk TA, Park R, Minear M, Savage A, Smith MR. Aging reduces neural specialization in ventral visual cortex. Proc Natl Acad Sci U S A. 2004;

54. Viana J, Hannon E, Dempster E, Pidsley R, Macdonald R, Knox O, et al.

Schizophrenia-associated methylomic variation: molecular signatures of disease and polygenic risk burden across multiple brain regions. Hum Mol Genet [Internet]. 2017;26(1):210–25. Available from: http://www.ncbi.nlm.nih.gov/pubmed/28011714

55. Numata S, Ye T, Herman M, Lipska BK. DNA methylation changes in the postmortem dorsolateral prefrontal cortex of patients with schizophrenia. Front Genet [Internet]. 2014;5:280. Available from: http://www.ncbi.nlm.nih.gov/pubmed/25206360

56. Pai S, Li P, Killinger B, Marshall L, Jia P, Liao J, et al. Differential methylation of enhancer at IGF2 is associated with abnormal dopamine synthesis in major psychosis. Nat Commun. 2019;

57. Ruzicka WB, Subburaju S, Benes FM. Circuit- and Diagnosis-Specific DNA Methylation Changes at gamma-Aminobutyric Acid-Related Genes in Postmortem Human Hippocampus in Schizophrenia and Bipolar Disorder. JAMA Psychiatry [Internet]. 2015;72(6):541–51. Available from: http://www.ncbi.nlm.nih.gov/pubmed/25738424

58. O'dushlaine C, Rossin L, Lee PH, Duncan L, Parikshak NN, Newhouse S, et al. Psychiatric genome-wide association study analyses implicate neuronal, immune and histone pathways. Nat Neurosci. 2015;

59. Chase KA, Rosen C, Rubin LH, Feiner B, Bodapati AS, Gin H, et al. Evidence of a sex-dependent restrictive epigenome in schizophrenia. J Psychiatr Res. 2015;

60. Fullard JF, Halene TB, Giambartolomei C, Haroutunian V, Akbarian S, Roussos P. Understanding the genetic liability to schizophrenia through the

neuroepigenome. Schizophrenia Research. 2016.

61. Hashimoto H, Vertino PM, Cheng X. Molecular coupling of DNA methylation and histone methylation. Epigenomics. 2010.

62. Du J, Johnson LM, Jacobsen SE, Patel DJ. DNA methylation pathways and their crosstalk with histone methylation. Nat Rev Mol Cell Biol. 2015;

63. Ooi SKT, Qiu C, Bernstein E, Li K, Jia D, Yang Z, et al. DNMT3L connects unmethylated lysine 4 of histone H3 to de novo methylation of DNA. Nature. 2007;

64. Singh T, Kurki MI, Curtis D, Purcell SM, Crooks L, McRae J, et al. Rare loss-of-function variants in SETD1A are associated with schizophrenia and developmental disorders. Nat Neurosci. 2016;

65. Tate CM, Lee JH, Skalnik DG. CXXC finger protein 1 restricts the Setd1A histone H3K4 methyltransferase complex to euchromatin. FEBS J. 2010;

66. Holtzman L, Gersbach CA. Editing the Epigenome: Reshaping the Genomic Landscape. Annu Rev Genomics Hum Genet. 2018;

67. Stricker SH, Köferle A, Beck S. From profiles to function in epigenomics. Nature Reviews Genetics. 2016.

68. Gibbs JR, van der Brug MP, Hernandez DG, Traynor BJ, Nalls MA, Lai SL, et al. Abundant quantitative trait loci exist for DNA methylation and gene expression in human brain. PLoS Genet [Internet]. 2010;6(5):e1000952. Available from: http://www.ncbi.nlm.nih.gov/pubmed/20485568

69. Castellani CA, Melka MG, Diehl EJ, Laufer BI, O'Reilly RL, Singh SM. DNA methylation in psychosis: insights into etiology and treatment. Epigenomics [Internet]. 2015;7(1):67–74. Available from:

http://www.ncbi.nlm.nih.gov/pubmed/25687467

70. Nishioka M, Bundo M, Koike S, Takizawa R, Kakiuchi C, Araki T, et al. Comprehensive DNA methylation analysis of peripheral blood cells derived from patients with first-episode schizophrenia. J Hum Genet [Internet]. 2013;58(2):91–7. Available from: http://www.ncbi.nlm.nih.gov/pubmed/23235336

71. Abdolmaleky HM, Pajouhanfar S, Faghankhani M, Joghataei MT, Mostafavi A, Thiagalingam S. Antipsychotic drugs attenuate aberrant DNA methylation of DTNBP1 (dysbindin) promoter in saliva and post-mortem brain of patients with schizophrenia and Psychotic bipolar disorder. Am J Med Genet Part B Neuropsychiatr Genet. 2015;

72. Joehanes R, Just AC, Marioni RE, Pilling LC, Reynolds LM, Mandaviya PR, et al. Epigenetic Signatures of Cigarette Smoking. Circ Cardiovasc Genet. 2016;9(5):436–47.

Figure 1

A

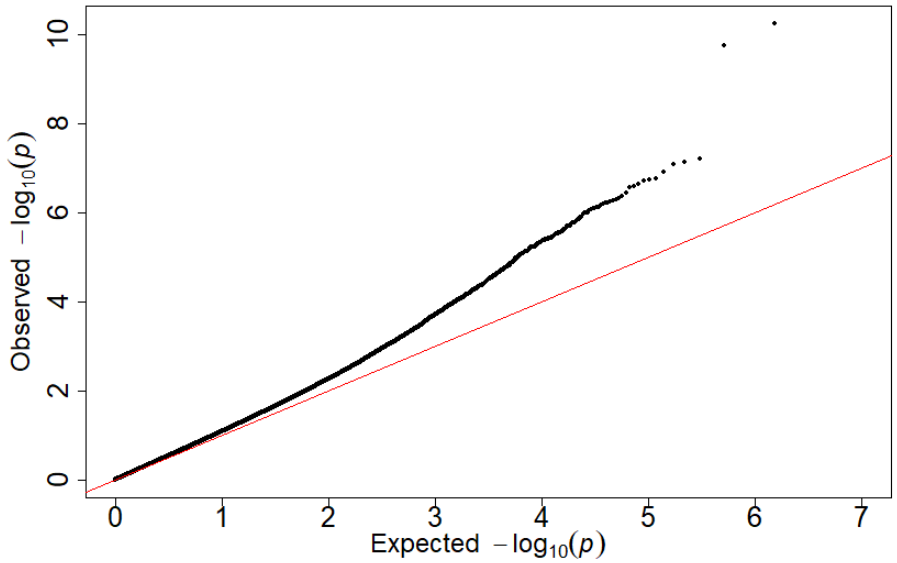
Observed $-\log_{10}(p)$
Expected $-\log_{10}(p)$
0
1
2
3
4
5
6
7
0
2
4
6
8
10

B

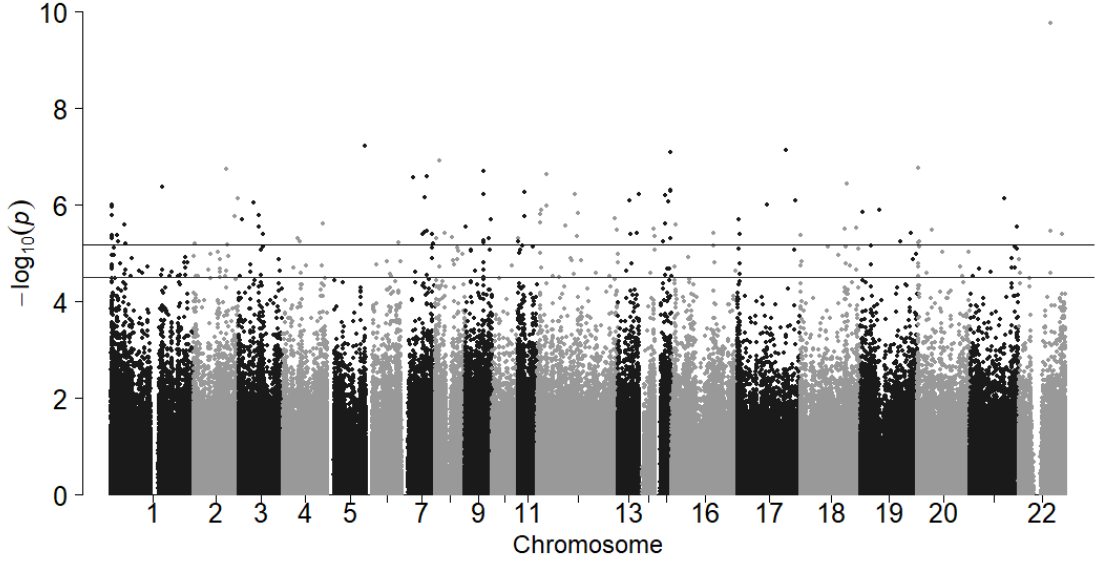
$-\log_{10}(p)$
Chromosome
0
2
4
6
8
10
1
2
3
4
5
7
9
11
13
16
17
18
19
20
22

Figure 2

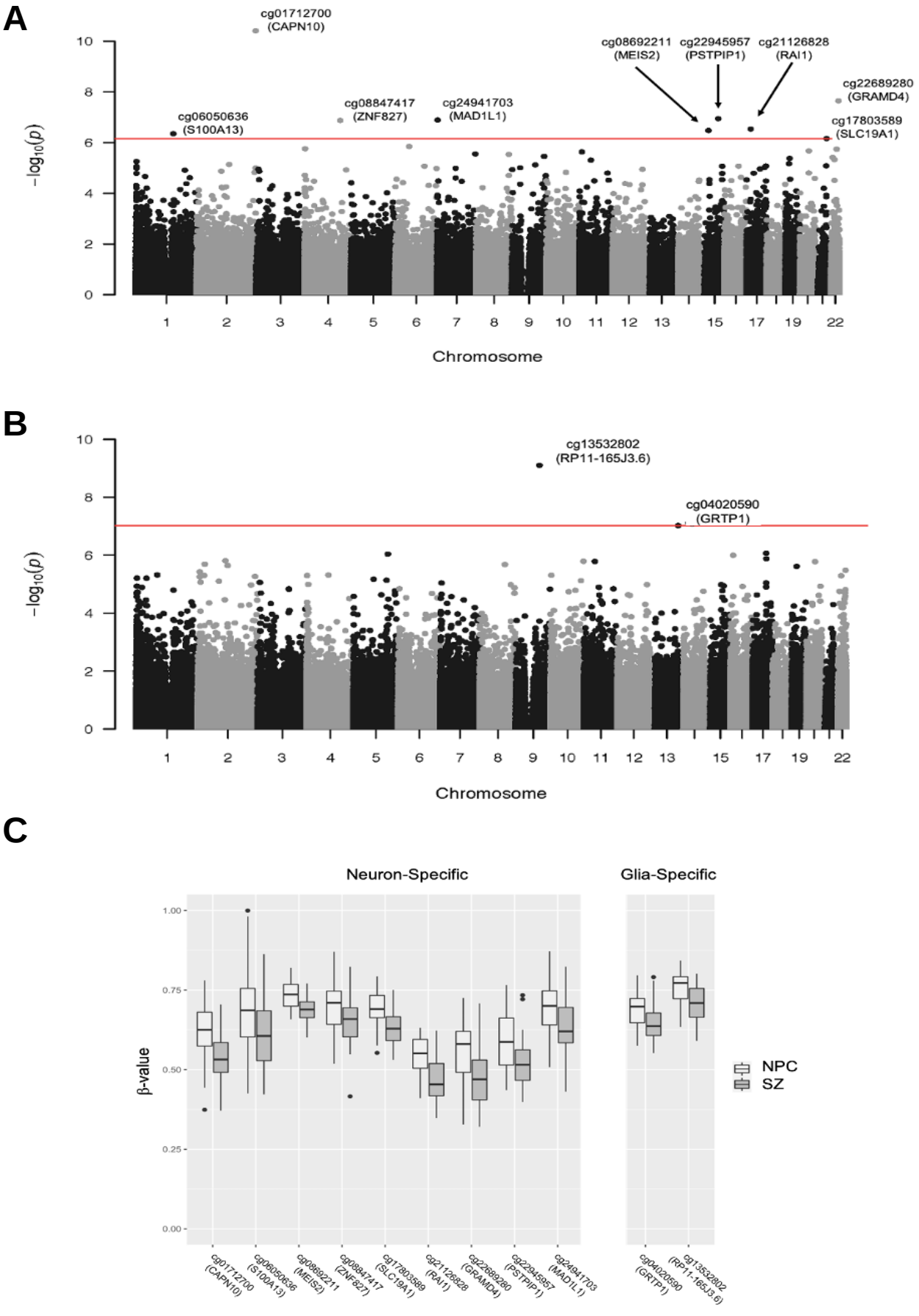

Table 1. Cohort characteristics

Group	*NPC*	*SZ*
Number	44	44
Sex	32M, 12F	31M, 13F
Race	35W, 8B, 1O	32W, 12B
Age (years)	48.25 ± 13.82	47.48 ± 13.88
PMI (h)	17.41 ± 5.89	18.32 ± 7.05
pH	6.70 ± 0.28	6.56 ± 0.31

Data for continuous variables are presented as group average ± standard deviation. Abreviations: B, black; DNAm, DNA methylation; F, female; M, Male; NPC, non-psychiatric comparison; O, other (Asian Indian); PMI, postmortem interval; SZ, schizophrenia; W, white.

Table 2. Differentially methylated sites in SZ. The 242 sites at which DNAm differed between SZ and NPC subjects with the FDR cutoff of q=0.1 (adjusted for age, race and PMI) are listed in the table. Abbreviations: DNAm, DNA methylation; NPC, non-psychiatric comparison; PMI, postmortem interval; SZ, schizophrenia.

Site	DNAm Difference (SZ-NPC; β-values)	q-value	Gene
cg01712700	-0.032	4.55E-05	CAPN10
cg13532802	-0.041	6.82E-05	
cg04020590	-0.032	0.013	GRTP1
cg08847417	-0.023	0.013	ZNF827
cg05621596	-0.018	0.013	GRAMD4
cg25079492	-0.028	0.016	CLEC16A
cg24941703	-0.028	0.017	MAD1L1
cg07748741	-0.012	0.017	UBTD1
cg23379913	-0.026	0.017	AKAP1
cg04011474	-0.028	0.018	
cg22945957	-0.028	0.018	PSTPIP1
cg08692211	-0.021	0.018	MEIS2
cg22519912	-0.027	0.022	PSD2
cg06050636	-0.035	0.024	S100A13
cg22689280	-0.029	0.024	
cg02478836	-0.022	0.024	TBC1D22A
cg26981306	-0.029	0.024	KIAA0892
cg13913915	-0.032	0.024	MSI2;MSI2
cg23453794	-0.032	0.024	MERTK
cg22348992	-0.016	0.024	CHRNA4
cg19261949	-0.024	0.024	ZMAT5
cg12349571	-0.018	0.024	TLE3
cg24158028	-0.028	0.024	STK32C
cg21265339	-0.023	0.024	
cg02289653	-0.025	0.024	EPB41L1
cg18282392	-0.019	0.024	GALNT7
cg25459000	-0.018	0.024	SYNGR1
cg19418922	-0.027	0.025	EXT2
cg02722031	-0.028	0.026	HERC3
cg01606571	-0.027	0.026	HADHA
cg03449456	-0.020	0.026	PRDM16
cg17601209	-0.032	0.026	PRDM16
cg12937501	-0.025	0.029	
cg10699522	-0.028	0.029	DST; LOC101930010
cg24920126	-0.022	0.031	PPP1R3G
cg23200394	-0.033	0.031	GLI2

cg12446793	-0.028	0.033	
cg25894668	-0.021	0.033	SLC3A2
cg07348768	-0.015	0.033	PRDM16
cg16901627	-0.020	0.033	COPE
cg00387200	-0.027	0.033	
cg21620968	-0.028	0.035	COPS7B
cg25211200	-0.026	0.035	MRVI1
cg20402747	-0.020	0.035	TBC1D16
cg13523224	-0.032	0.035	CFAP99
cg06022867	-0.043	0.038	
cg15044372	-0.025	0.039	
cg24318537	-0.024	0.039	UNC119B
cg21408848	-0.026	0.040	IQSEC1
cg12713481	-0.027	0.040	
cg21946195	-0.034	0.040	ATOH8
cg09815962	-0.027	0.041	EIF2C2
cg14608424	-0.025	0.041	ABR
cg24512544	-0.021	0.041	EIF2C2
cg17134838	-0.023	0.041	
cg18329758	-0.027	0.041	WWC1
cg13689085	-0.026	0.041	TCF7
cg16266918	-0.024	0.041	PDXK
cg23634532	-0.023	0.042	OGDH
cg16433632	-0.014	0.043	RAMP1
cg14517390	-0.019	0.043	ACSBG1
cg07605200	-0.026	0.043	
cg19788036	-0.026	0.043	
cg02347483	-0.022	0.043	CCDC101
cg01433955	-0.028	0.043	
cg00686823	-0.024	0.043	TPRA1
cg08419879	-0.018	0.043	PLEKHG1
cg03595140	-0.027	0.043	FNBP1
cg21785920	-0.038	0.043	LBP
cg25298833	-0.027	0.043	RGMA
cg01287037	-0.028	0.043	
cg03932760	-0.022	0.043	ARRB1; MIR326
cg14372037	-0.030	0.043	SORCS2
cg15165927	-0.024	0.043	NKD2
cg25601830	-0.022	0.043	AKR7A2
cg01203812	-0.026	0.043	PRDM16;
cg17803589	-0.023	0.043	SLC19A1
cg15845746	-0.012	0.043	TMEM177
cg27151770	-0.022	0.045	ZNF423

cg26520908	-0.028	0.045	PRDM16
cg04500745	-0.017	0.045	MAPK8IP3
cg14020176	-0.020	0.045	SLC9A3R1
cg04633409	0.019	0.045	TWF1
cg07597386	-0.007	0.045	PRDM16
cg00159552	-0.018	0.045	TBC1D22A
cg26632239	-0.014	0.045	CTDP1
cg13136596	-0.034	0.048	MSI2
cg24883899	-0.018	0.048	APC2
cg16023894	-0.030	0.048	EPHB2
cg16011164	-0.028	0.048	MIR4656; AP5Z1
cg00162902	-0.019	0.048	FAM184A
cg09925572	-0.025	0.048	TFCP2
cg17529670	-0.022	0.048	BCR
cg01123449	-0.026	0.048	HHIPL1
cg18783374	-0.024	0.048	MSI2
cg16622899	0.020	0.048	MAFK
cg08256119	-0.025	0.048	MSI2
cg14297573	-0.032	0.049	PFKP
cg12590902	-0.022	0.049	ERI3
cg06317803	0.018	0.049	
cg05068943	-0.019	0.049	
cg24338094	-0.022	0.052	PLXNA1
cg22649529	-0.035	0.053	TECR
cg19736604	-0.024	0.053	TNXB
cg01952185	0.019	0.053	
cg05501958	-0.011	0.053	APOE
cg26409376	-0.032	0.053	
cg04618897	-0.028	0.053	KIAA0415
cg08209664	-0.020	0.053	ST3GAL1
cg24484600	-0.022	0.053	GDPD5
cg07987705	-0.021	0.053	RGMA
cg15728120	-0.018	0.053	CENPT
cg09788030	-0.025	0.053	
cg08425757	-0.012	0.055	TRAPPC9
cg08196145	-0.018	0.055	
cg07463740	-0.025	0.055	
cg11301187	-0.025	0.055	KIAA0195
cg27214458	-0.012	0.055	MRGPRF; MRGPRF-AS1
cg23879743	-0.019	0.055	
cg03629926	-0.020	0.055	ANGPTL4
cg21126828	-0.027	0.056	RAI1
cg20108328	-0.024	0.056	C21orf70

cg23564627	-0.023	0.057	PEMT
cg07504768	-0.022	0.057	MTSS1L
cg22548266	-0.026	0.058	SPOCK2
cg04792024	-0.024	0.059	TMEM120A
cg13259703	-0.022	0.059	
cg19177744	-0.024	0.059	
cg12985235	-0.010	0.059	MPND
cg15343406	-0.038	0.061	
cg04594439	-0.025	0.061	PASK
cg17282060	-0.012	0.061	ARHGAP22
cg17196564	-0.020	0.062	
cg13175786	-0.022	0.062	PRDM16
cg09214323	-0.024	0.062	RNU6-2; KIF1B
cg08213909	-0.026	0.063	MCC
cg17736422	-0.034	0.063	PRDM16
cg26201596	0.026	0.065	
cg15748271	-0.020	0.065	TRIM8
cg17320669	-0.026	0.066	CAPN2
cg26301507	-0.018	0.068	SLC25A20
cg05141465	-0.026	0.069	CHST10
cg03950655	-0.021	0.069	ROR1
cg03628962	-0.021	0.069	RGMA
cg13821176	-0.029	0.069	TRIB1
cg15365305	-0.021	0.070	SMARCA2
cg10225499	-0.031	0.070	EZR
cg15412087	-0.024	0.070	OAF
cg03957687	-0.024	0.070	CENPT
cg01053681	-0.027	0.070	ZMIZ1
cg00726470	-0.017	0.071	
cg06520014	-0.016	0.071	
cg18069081	-0.025	0.072	GPR39
cg03272941	-0.020	0.073	RHOJ
cg26122413	-0.019	0.075	INF2
cg05071292	-0.013	0.075	LOC728613
cg11197533	-0.025	0.076	IFT122
cg26000554	-0.023	0.076	MOSC2
cg21036560	-0.024	0.076	PGBD5
cg12441066	-0.026	0.076	MSI2
cg08589214	-0.023	0.076	CAPN10
cg05878289	-0.023	0.076	SORCS2
cg04964562	-0.016	0.076	PLCG1
cg25619978	0.017	0.076	TRPC7
cg03747028	0.011	0.077	TAF12

cg06847567	0.019	0.078	
cg02133510	-0.023	0.078	TNXB
cg12863924	-0.026	0.078	
cg24379495	-0.021	0.078	SLC1A2
cg17823326	-0.017	0.079	NUBPL
cg26489368	-0.023	0.079	NKD2
cg20988960	-0.030	0.079	PRDM16
cg25456772	0.017	0.079	RAB3IP
cg04844692	-0.021	0.079	C12orf49
cg08067895	-0.024	0.079	CDX1
cg13153666	-0.022	0.080	
cg14597213	-0.021	0.082	AHCYL1
cg09792192	-0.017	0.082	AHCYL2
cg25122824	-0.017	0.082	MAD1L1
cg07410783	-0.025	0.082	CLEC16A
cg15763706	-0.026	0.082	SRGAP3
cg13547132	-0.020	0.082	
cg02986801	-0.019	0.083	ST3GAL1
cg11569621	-0.019	0.084	
cg26051775	-0.019	0.084	CAPN2
cg24986651	-0.023	0.084	LPIN1
cg01419991	-0.022	0.085	TRIB1
cg02743070	-0.019	0.085	ZMIZ1
cg05808227	-0.024	0.085	
cg06714043	-0.040	0.085	
cg09509365	-0.020	0.085	PRDM16
cg05321174	-0.014	0.086	PTK2B
cg00305491	-0.026	0.088	WWC1
cg22738000	-0.014	0.088	RASSF4
cg15900987	-0.016	0.088	BGLAP
cg07580832	-0.021	0.088	MSI2
cg19710386	-0.022	0.088	PTPRF
cg24699097	-0.016	0.089	RAB11FIP4
cg09761288	-0.023	0.089	
cg09255521	-0.033	0.090	
cg17877405	-0.025	0.090	CST3
cg15232718	-0.028	0.090	UBTD1
cg22177068	-0.028	0.090	ATP13A4-AS1; ATP13A4
cg17214089	-0.024	0.090	GLUL
cg00659252	-0.017	0.090	ASPH
cg13904892	-0.019	0.090	C15orf62; DNAJC17
cg08333580	-0.019	0.090	SLC1A2
cg26654807	0.015	0.091	ZMIZ1

cg11047279	-0.021	0.092	
cg18773993	-0.022	0.093	ABCA4
cg07380086	-0.024	0.093	CHN1
cg05912181	-0.019	0.093	LOC100506497
cg05747038	-0.018	0.093	GLIS3
cg17505776	-0.015	0.093	ITSN1
cg09676376	-0.023	0.094	ZNF385A
cg21184699	-0.020	0.094	FAM120A
cg24186251	-0.023	0.094	SH3RF3
cg13721930	-0.018	0.094	
cg15395783	-0.022	0.096	HEYL
cg21148160	-0.028	0.096	PAPLN
cg10782534	0.015	0.097	
cg23919411	-0.025	0.097	SEC14L4
cg12480689	-0.024	0.097	PFKFB2
cg16028934	-0.008	0.097	TP53BP2
cg21049762	-0.027	0.097	TCIRG1
cg10589385	0.056	0.097	SETDB1
cg06873567	-0.023	0.098	
cg13461192	-0.024	0.098	RHOQ
cg12128274	0.028	0.098	CNOT4
cg13691436	-0.023	0.098	FRMD4A
cg02276845	-0.006	0.098	STIM1
cg10051022	-0.015	0.098	FGGY
cg17876641	-0.025	0.098	KIF21B
cg19705197	-0.021	0.098	PFKFB3
cg03718662	-0.020	0.098	RASAL2
cg25307778	-0.021	0.098	ERI1
cg13302567	-0.024	0.098	MAD1L1
cg25674846	-0.018	0.098	LOC100506603; ANGEL1
cg00104333	-0.019	0.098	LGI1
cg07303829	-0.019	0.098	PPP6R2
cg02752163	0.043	0.098	
cg17931415	-0.028	0.098	MSI2

Table 3. Differentially methylated regions in SZ. The 44 genomic regions in which DNAm differed at two or more contiguous, measured sites between SZ and NPC subjects are listed . Abbreviations: DNAm, DNA methylation; DMR, differentially methylated region; SZ, schizophrenia; NPC, non-psychiatric comparison; bp, base pairs.

Chromosome	Start	End	Length in bp	Number of Significant Probes	Mean β-value Coefficent	Overlapping Promoters	Overlapping Genes
6	28828946	28829503	557	15	0.012562318	LINC01623, RPL13P	LINC01623, RPL13P
1	16062361	16063471	1110	11	-0.010632242	SLC25A34, RP11-288I21.1	SLC25A34, RP11-288I21.1
1	3191219	3192542	1323	10	-0.021685336		PRDM16
10	6263235	6264776	1541	9	-0.016688209	PFKFB3	PFKFB3
19	48958216	48959043	827	9	-0.014250403	KCNJ14	GRWD1
15	93617080	93617833	753	9	-0.016227133	RGMA	RGMA
1	2999586	3001128	1542	8	-0.020050418		PRDM16
4	1800154	1801294	1140	8	-0.012881307	FGFR3	FGFR3
3	187453721	187454786	1065	8	-0.015068722	BCL6	BCL6
3	13082751	13083684	933	7	-0.018337881		IQSEC1
1	153600597	153600972	375	7	-0.016748303	S100A1, S100A13	S100A1, S100A13
3	12949457	12950513	1056	6	-0.015753296		IQSEC1
4	1803298	1805090	1792	6	-0.015286045	FGFR3	FGFR3
8	141588118	141588943	825	6	-0.017229636		AGO2
2	8711042	8711256	214	6	-0.018511245		LINC01814
4	1807819	1808646	827	6	-0.01256232	FGFR3	FGFR3
4	866299	866811	512	6	-0.017785773	GAK	GAK
14	21491808	21492316	508	6	-0.010876489	NDRG2	NDRG2
10	99329961	99330447	486	5	-0.014591035	ANKRD2	UBTD1
2	241535685	241536284	599	5	-0.021733676	CAPN10	CAPN10
1	3154081	3154700	619	5	-0.023621906	PRDM16	PRDM16
5	1033518	1034076	558	4	-0.023946075	NKD2	NKD2
19	45411802	45412647	845	4	-0.023104719		APOE
7	2262244	2262479	235	4	-0.020981488	MAD1L1	MAD1L1
6	5087031	5087749	718	4	-0.021469791	PPP1R3G	PPP1R3G, LYRM4
9	138966848	138967347	499	4	-0.021449114		NACC2
10	7212815	7213304	489	4	-0.021980366		SFMBT2
12	117157450	117158154	704	4	-0.015498341	C12orf49	C12orf49
10	3162054	3162191	137	4	-0.017789142		PFKP
13	79170146	79170430	284	4	0.014049989		OBI1-AS1
9	96199463	96199581	118	3	-0.02791665	RP11-165J3.6-001	
17	55703709	55704098	389	3	-0.029515629		MSI2
5	167858238	167858326	88	3	-0.017722017	WWC1-008, WWC1-007	WWC1
22	47016623	47017522	899	3	-0.020100319	GRAMD4	GRAMD4
17	79686849	79687075	226	3	-0.026164519		SLC25A10
1	223945127	223945297	170	3	-0.022033434	CAPN2	CAPN2
1	3128606	3129115	509	3	-0.024216925		PRDM16
15	93611859	93611950	91	2	-0.024325293		RGMA
7	4829256	4829350	94	2	-0.028189732	AP5Z1, MIR4656	AP5Z1
15	70364327	70364359	32	2	-0.020032632		TLE3
15	65594642	65594648	6	2	-0.024798094	PARP16	RP11-349G13.2
14	65689711	65689836	125	2	-0.021050816	LINC02324	
17	77954963	77955167	204	2	-0.0173864		TBC1D16
3	58558333	58558343	10	2	-0.018019101	RP11-475O23.2	FAM107A